Magnitude and Origin of the Anthropogenic CO_2 Increase and ^{13}C Suess Effect in the Nordic Seas Since 1981

Are Olsen[1,2*], Abdirahman M. Omar[2,1], Richard G.J. Bellerby[2,1], Truls Johannessen[1,2], Ulysses Ninnemann[3,2], Kelly R. Brown[2], K. Anders Olsson[2,1], Jon Olafsson[4], Gisle Nondal[1], Caroline Kivimäe[1], Solveig Kringstad[1], Craig Neill[2], Solveig Olafsdottir[4]

[1]Geophysical Institute, University of Bergen, Norway.
[2]Bjerknes Centre for Climate Research, University of Bergen, Norway.
[3]Departement of Earth Science, University of Bergen, Norway.
[4] University of Iceland and Marine Research Institute, Reykjavik, Iceland.

[*]Corresponding author. Tel: (+47) 55584322, fax: (+47) 55584330, e-mail: are.olsen@gfi.uib.no

Abstract

This study evaluates the anthropogenic changes of CO_2 (ΔC_{ant}) and $\delta^{13}C$ ($\Delta\delta^{13}C_{ant}$) in the Nordic seas, the northern limb of the Atlantic Meridional Overturning Circulation, that took place between 1981 and 2002/03. The changes have been determined by comparing data obtained during the Transient Tracers in the Ocean, North Atlantic Study (TTO-NAS) with data obtained during the Nordic seas surveys of R/V *Knorr* in 2002 and R/V *G.O. Sars* in 2003 using an extended multi-linear regression approach. The estimated $\Delta\delta^{13}C_{ant}$ and ΔC_{ant} and their relationship to each other and to water mass distribution suggest that the Polar Water entering the Nordic seas from the north is undersaturated with respect to the present atmospheric anthropogenic CO_2 levels and promotes a local uptake of C_{ant} within the Nordic seas. In contrast, the Atlantic Water entering from the south appears equilibrated. It carries with it anthropogenic carbon which will be sequestered at depth as the water overturns. This pre-equilibration leaves no room for further uptake of C_{ant} in the parts of the Nordic seas dominated by Atlantic Water. The upper ocean pCO_2 in these regions appears to have increased at a greater rate than the atmospheric pCO_2 over the last two decades; this is reconcilable with a large lateral advective supply of C_{ant}.

1. Introduction

The increase of the atmospheric CO_2 concentration caused by fossil fuel combustion, cement production, and land use change is significantly dampened by oceanic CO_2 uptake. Current annual net oceanic CO_2 uptake corresponds to roughly one quarter of the fossil fuel and cement manufacturing emissions [*Prentice et al*., 2001], and the accumulated oceanic uptake since the start of the industrial revolution corresponds to approximately 50% of the emitted fossil CO_2 [*Sabine et al*., 2004]. The size of the oceanic inventory of anthropogenic carbon (C_{ant}) is, however, hard to estimate due to the absence of oceanic carbon observations from the pre-industrial era and estimates such as the quoted *Sabine et al.* [2004] have to rely on indirect approaches [*Gruber et al.*, 1996] with inherent methodological uncertainties. Our understanding of where and when C_{ant} is taken up by the oceans, how it is transported within them, and where it is stored is therefore uncertain. This situation is now being alleviated by continued observations which enable us to observe and quantify carbon concentration changes in the interior ocean associated with C_{ant} input.

Decadal changes have been quantified in the Pacific Ocean [*Peng et al.,* 2003], the Indian Ocean [*Peng et al*., 1998; *Sabine et al*., 1999], and in the Southern Ocean [*McNeil et al.*, 2001a] by comparing recent carbon data with the data collected during GEOSECS and other expeditions that were carried out during the 1960s and 1970s. In the present paper observations obtained during the Transient Tracers in the Ocean, North Atlantic Study (TTO-NAS) of 1981 are compared with data obtained during two recent surveys of the Greenland, Iceland, and Norwegian Seas. This allows for the quantification and increased understanding of the C_{ant} input to the northernmost parts of the Atlantic Ocean over the last two decades.

The Greenland, Iceland, and Norwegian Seas, collectively known as the Nordic seas, are considered important for the natural exchange of carbon between the ocean and the

atmosphere, representing the pre-industrial carbon fluxes. Annually, approximately 6 Sv (Sverdrup, 10^6 m^3 s^{-1}) of warm and salty Atlantic Water (AW) from further south enter the region [*Hansen and Østerhus*, 2000]. This water is cooled and transformed to subsurface waters within the Nordic seas themselves, and also in the Arctic Ocean and associated shelf areas. The subsurface waters exit the Nordic seas over the Greenland-Scotland ridge and contribute to a total northern North Atlantic overturning circulation of 15 Sv [*Álvarez et al.*, 2002]. The cooling of the northward flowing AW drives a flux of CO_2 from the atmosphere into the ocean so that the waters that overturn in the Nordic seas and contribute to the global oceanic deep water pool are loaded with carbon. As the waters eventually upwell this carbon is released back to the atmosphere, along with carbon that was added to the deep water from decaying organic material.

The Nordic seas are also considered an important region for oceanic uptake of C_{ant}. The air-sea flux of anthropogenic CO_2 is not driven by biology and meridional water transport as the pre-industrial air-sea CO_2 flux, but by the increase of the atmospheric CO_2 concentration which has perturbed the natural exchanges between the ocean and the atmosphere. Given approximately one year the surface layer of the world oceans will equilibrate with the atmosphere [*Broecker and Peng*, 1974] and further uptake will rely on exposure of older water to the atmosphere. The largest air-to-sea transfer of C_{ant} is thus considered to take place in regions with extensive communication between surface and deep waters such as the tropical and Southern Ocean upwelling regions and the North Atlantic convection areas. A large air-to-sea flux of anthropogenic CO_2 and an efficient surface-to-deep ocean carbon transport is expected to occur in the Nordic seas. Indeed, with respect to the latter, C_{ant} estimates do reveal deep penetration in the Nordic seas spreading into the deep Atlantic [*Gruber et al*., 1998; *Sabine et al*., 2004]. As regards the air-sea flux of anthropogenic carbon on the other hand, the situation is somewhat unclear. Three dimensional ocean carbon cycle

models do tend to show a large air-sea C_{ant} flux in the northern North Atlantic and Nordic seas [*Orr et al.*, 2001; *Wetzel et al*., 2005], but these results have, however, recently been challenged by estimates of oceanic C_{ant} transport which seem to agree that the largest uptake of C_{ant} takes place in the tropical-to-subtropical Atlantic, so that the waters that enter the subpolar regions are already equilibrated with the atmosphere's anthropogenic CO_2 concentration, leaving little room for further uptake [*Álvarez et al*., 2003; *Macdonald et al*., 2003; *Rosón et al*., 2003]. In fact, the *Rosón et al.* [2003] estimate indicates that the subtropical-to-subpolar Atlantic is a source of anthropogenic CO_2 to the atmosphere; that is, the uptake of CO_2 from the atmosphere has been reduced since pre-industrial times. This result is in agreement with output from simple model calculations [*Wallace*, 2001; *Anderson and Olsen*, 2002; *Bellerby et al*., 2005]. Observations from the North Atlantic do indeed seem to verify that the surface ocean pCO_2 in this area has increased at a greater rate than the atmospheric pCO_2 over the last 20 years [*Lefèvre et al*., 2004], implying a reduced uptake of atmospheric CO_2. However, the extent to which this increase is a consequence of anthropogenic CO_2 or of biological and/or temperature effects was not resolved by *Lefèvre et al*. [2004]. Surface ocean pCO_2 appears to have increased in the Barents Sea as well, as presented by *Omar et al*. [2003]. They applied an approach that accounted for changes in biology and hydrography, so their estimated annual mean increase of 1.3 μatm yr^{-1} between 1967 and 2001 is solely due to anthropogenic carbon. This increase is slightly lower than the atmospheric increase of 1.4 μatm yr^{-1} in the same time interval. Since no gradients could be observed within the Barents Sea, the authors suggested that the anthropogenic carbon had been advected into the region from the Nordic seas.

This paper focuses on the region between the areas addressed by *Lefévre et al.* [2004] and *Omar et al*. [2003]: the Nordic seas. The area was surveyed during the summers of 2002 and 2003 using R/V *Knorr* and R/V *G.O. Sars*. Data describing the inorganic carbon system were

acquired during both cruises as well as data for temperature, salinity, and nutrient concentrations. These data are compared with the data acquired in the same area during the TTO-NAS of the summer of 1981, aiming to determine the changes of the C_{ant} concentrations over the two decades that separate these surveys. To this end an extended version of the multi-linear regression (MLR) approach of *Wallace* [1995] is employed, the eMLR approach as first introduced by *Sonnerup et al.* [2000] and later formalized by *Friis et al.* [2005]. The eMLR method is also employed on data of the ^{13}C-to-^{12}C ratio, $\delta^{13}C$, acquired during the TTO-NAS and the *Sars* cruises so that the magnitude of the oceanic ^{13}C Suess effect in the region and its relationship with the anthropogenic CO_2 changes can be estimated. The ^{13}C Suess effect is a consequence of the fact that fossil fuel CO_2 is relatively enriched with the light carbon isotope ^{12}C so that emissions lead to a decrease of the ^{13}C-to-^{12}C ratio in the atmosphere. Isotopic exchange across the air-sea interface transmits this perturbation to the ocean, giving rise to the oceanic ^{13}C Suess effect. Information on the magnitude of this effect can be used to quantify oceanic uptake of C_{ant} [*Quay et al*., 1992; *Tans et al*., 1993; *Heimann and Maier-Reimer*, 1996; *Quay et al*., 2003], and the ratio of oceanic C_{ant} and ^{13}C changes provides information on the recent atmospheric exposure histories of water masses [*McNeill et al*., 2001b; *Körtzinger et al*., 2003].

2. Data and Methods

The positions of the data used in the present work are presented in Figure 1. Data selection has been limited to offshore of the 250 m isobath to avoid coastal influence, and at/or north of the Greenland-Scotland ridge.

2.1 TTO-NAS Data

The TTO-NAS was carried out from April to October of 1981. The TTO-NAS survey consisted of 7 legs and the Nordic seas were surveyed during leg 5, in late July and early August. The data used here were acquired at stations 142 to 159. The data were obtained from the Carbon Dioxide Information Analysis Center (CDIAC), Oak Ridge, Tennessee, USA. The total concentration of inorganic carbon (Ct) in water was determined at sea as well as on shore after the cruise. The at-sea determinations were carried out using potentiometric titration while the on-shore determinations were carried out in the late Dr. C.D. Keeling's laboratory at Scripps Institution of Oceanography using the gas extraction manometric technique described by *Weiss et al.* [1982]. Subsequent analyses revealed that the Ct values determined at sea were higher than the values determined on shore. This motivated the release of a revised TTO Ct dataset which was calculated from the TTO total alkalinity (TA) and pCO_2 data using the carbon system constants of *Merbach et al*., [1973] [*Brewer et al*., 1986]. Recently *Tanhua and Wallace* [2005] have reanalyzed the TTO carbon chemistry data from legs 2, 3, 4, and 7. They find that the TTO TA data are biased high with respect to modern data tied to Certified Reference Material (CRM) and recommend that they should be adjusted down by 3.6 μmol kg^{-1}. They moreover recommend that the TTO Ct values should be recalculated using the adjusted TA data and currently accepted constants and then adjusted upwards by 2.4 μmol kg^{-1} based upon comparison with the manometric Ct values obtained during TTO. These recommendations were followed in the present work. Leg 5 Ct values thus computed were on average 0.26 μmol kg^{-1} higher than the manometric data; this compares favorably to the offset between the manometric and revised Ct data of 2.5 μmol kg^{-1}, the latter being lower.

The TTO-NAS data of the ^{13}C-to-^{12}C ratio of dissolved inorganic carbon, $\delta^{13}C$, were acquired from CDIAC. The data were measured by the Carbon Dioxide Research Group at Scripps Institution of Oceanography using procedures described by *Gruber et al.* [1999]. All data that were flagged as suspicious in the original data set were discarded, as well as data points where

the replicate analyses differed by more than three times the estimated combined error from sampling and analysis, 0.12‰ (3X0.04‰), following *Gruber et al*. [1999].

2.2 R/V *Knorr* Data

The R/V *Knorr* cruise was carried out in June 2002 and covered most regions of the Nordic seas (Figure 1). The temperature, salinity, and nutrients data acquired during this cruise will be described by *Bellerby et al.* [manuscript in preparation 2005]. The data for Ct that are employed here were determined by gas extraction of acidified water samples followed by coulometric titration [*Johnson et al*., 1985, 1987]. The accuracy was set by running CRM supplied by Andrew Dickson of Scripps Institution of Oceanography, and the precision has been determined to better than ± 2 μmol kg^{-1} by comparison of deep samples acquired in the western Greenland basin where the Ct is regarded as being homogenous [*Bellerby et al*., manuscript in preparation, 2005].

2.3 R/V *G.O. Sars* Data

The R/V *G.O. Sars* cruise was carried out from September to October of 2003. The cruise covered the Barents Sea Opening, the Greenland Sea, the Faeroe-Shetland Gap, the Faeroe Bank Channel, and the Svinøy Section that extends NW off the coast of Norway from 62ºN. Data were also acquired at a few stations in the Iceland Sea (Figure 1). Temperature and salinity data were obtained using a SBE 911*plus* CTD profiler. The initial accuracy of the conductivity and temperature sensors were 0.0003 S/m and 0.002°C, respectively. The CTD profiler carried two temperature and two conductivity sensors and the standard deviation of each pair of sensors averaged over all stations was 0.0023°C for temperature and 0.0012 for salinity. The CTD salinity data were corrected to bottle samples by a polynomial fit. The

standard deviation of the difference between the CTD and the bottle values was 0.0047 with a correlation coefficient of 0.9998.

The nitrate and silicate data were analyzed on the ship using a Chemlab 3-channel autoanalyser following methods of *Grasshoff* [1970]. Phosphate was analyzed using a modified version of the *Murphy and Riley* [1962] method. The accuracy and precision of the nutrient analyses have been assessed by running nutrient test samples supplied by the QUASIMEME program [*Wells et al*., 1997] and laboratory reference material [*Aminot and Kéroue*l, 1998]. The laboratory reference material was run at each station and indicates precisions (1 σ) of ± 0.13 μmol kg^{-1} for nitrate, ± 0.02 μmol kg^{-1} for phosphate, and ± 0.27 μmol kg^{-1} for silicate over the duration of the cruise. Immediately after the cruise the laboratory reference material was analysed together with test samples from the QUASIMEME programme. The test sample results were in very good agreement with the QUASIMEME assigned values.

Ct was determined using the same method as during the *Knorr* 2002 cruise. Accuracy was set by running CRM as for the *Knorr* cruise. The combined sample handling and measurement error of these data were determined to be 0.4 μmol kg^{-1} by analyzing samples drawn from ten different Niskin bottles closed at the same depth (1 σ).

The $\delta^{13}C$ samples acquired on this cruise were collected in 100-ml bottles and poisoned with $HgCl_2$ and sealed with rubber stoppers immediately after collection. The samples were stored cold and in the dark. Each sample was analyzed in triplicate using a Finnigan GasBench coupled to a Mat 252 mass spectrometer within three months of the cruise. Based on 16 samples taken below 2000 m in the Greenland Sea with very similar physical and chemical water mass characteristics, the precision has been determined to be at least ± 0.07‰ (1 σ) for these results, just above the long term precision of the machine based on standard replicates (± 0.05‰).

2.4 eMLR Calculations

The extended multi-linear regression (eMLR) approach builds on the multi-linear regression (MLR) approach for determining C_{ant} changes introduced by *Wallace* [1995] and subsequently employed on several occasions [*Sabine et al*., 1999; *McNeil et al.*, 2001a; *Peng et al.,* 2003]. The MLR method has also been used to determine the oceanic ^{13}C Suess effect in the Southern Ocean [*McNeil et al.*, 2001b]. The underlying idea of this method is that whereas the carbon system in itself is perturbed as C_{ant} enters the ocean, the natural variations can be accounted for using a number of predictive parameters such as salinity, temperature, apparent oxygen utilization (AOU), nutrients, TA, etc. The approach takes advantage of the fact that changes of the C_{ant} concentration will affect the accuracy of empirically derived functions that estimate Ct, provided the predictive parameters are only influenced by natural processes. The MLR method applies an equation, derived for one region with data obtained at one time, to predict Ct concentrations using data obtained in the same region but at a different time. Any systematic bias revealed through comparing measured with predicted Ct values is ascribed to changes in the concentration of C_{ant}. The eMLR technique was first introduced by *Sonnerup et al*. [2000] for $\delta^{13}C$ data. Later on *Friis et al*. [2005] further formalized and reviewed the eMLR technique for Ct data. Rather than evaluating the offset between measured and predicted Ct values, the eMLR technique employs two regression equations derived from two data sets collected at different times. The two equations are applied on one set of predictive variables and differences in the predicted Ct values reveal the C_{ant} change. This method minimizes the measurement error associated with the independent variables since they enter the prediction twice, once when they are employed in the modern relationship and once when they are employed in the historical relationship [*Friis et al*., 2005].

The predictive equations for Ct and $\delta^{13}C$ were derived using salinity, potential temperature (θ), nitrate, and silicate as independent variables. These parameters were found to be sufficient and necessary. Adding the parameters AOU and TA did not improve the fit. Nitrate data were preferred to phosphate as comparison of the phosphate data collected at the *Knorr* and *Sars* cruises revealed significant differences in deep waters, ~0.2 μmol kg^{-1}, indicating issues with the phosphate analyses on one of the cruises. There were no significant deep water differences between these cruises with respect to the other variables used in this study. A cut-off value of 0.5 μmol kg^{-1} was applied to the nitrate data to avoid the potential impact of carbon overconsumption at very low nutrient levels [*Falck and Anderson*, 2005]. The regression analyses were carried out using the software package R [*R Development Core Team*, 2004]. The coefficients and statistics of each relationship are listed in Table 1. The residuals are plotted as a function of fitted values in Figure 2 a and b, and versus depth in Figure 3 a and b. In general the relationships predict Ct and $\delta^{13}C$ to within ± 6 μmol kg^{-1} and ± 0.07‰ as evaluated from the root mean square (rms) values (Table 1). The accuracy of the Ct relationships appears uniform over the whole range of Ct values as evaluated from Figure 2. The predictions are biased slightly high deeper than 2000 m, around 1 to 2 μmol kg^{-1}, with the TTO results being higher (Figure 3). Precision of the Ct predictions appears stable with depth to ± 5 μmol kg^{-1}; this is taken as a measure of the uncertainty of the C_{ant} estimates, except in the upper 100 m where precision decreases to ± 10 μmol kg^{-1}. The precision of the $\delta^{13}C$ predictions appears to be within an acceptable ± 0.1‰ at all depths, but it was not possible to evaluate deep TTO precisions due to the limited number of samples.

The anthropogenic changes of C_{ant} (ΔC_{ant}) and $\delta^{13}C$ ($\Delta\delta^{13}C_{ant}$) were estimated as the difference between *Knorr/Sars* equations and the TTO equations when both were applied to the TTO data. The equations were employed on the TTO data because these data define the region where all of the regression equations are known to be valid. Moreover, ΔC_{ant} was only

determined for samples within the salinity, θ, nitrate, and silicate ranges for which both the *Knorr/Sars* and the TTO relationships were valid, i.e., the common validity range. The same was the case for the $\Delta\delta^{13}C_{ant}$ estimates. These ranges are provided in Table 2.

3. Hydrographic Setting

A description of the hydrographic features of the TTO section is necessary before considering the results of the ΔC_{ant} and $\Delta\delta^{13}C_{ant}$ calculations. The one presented here is based on the more comprehensive descriptions of the hydrography of the Nordic Seas by *Hopkins* [1991], *Hansen and Østerhus* [2000], *Rudels et al*. [2005], and *Blindheim and Østerhus* [2005].

A schematic of the Nordic seas upper ocean circulation is presented in Figure 4. It is dominated by the northward flow of warm and saline AW in the east and the southward flow of fresher and colder Polar Water (PW) from the Arctic Ocean in the west. These water types meet and mix in the area between and form Arctic Surface Water, and as this water is cooled during winter several types of Arctic Intermediate Water (ArIW) are formed. The deep waters are not only formed locally such as Greenland Sea Deep Water (GSDW), but are also advected into the region from the Arctic Ocean. Canadian Basin and Eurasian Basin Deep Waters enter the Nordic seas through the Fram Strait, meet and mix with GSDW and moves south into the deep Lofoten and Norwegian basins as Norwegian Sea Deep Water (NSDW).

The distributions of temperature and salinity along a south-to-north section based on the TTO data are displayed in Figure 5. The positions of the stations have been specified in Figure 4. The upper 600 meters of the southernmost station (Sta. 142) in the Faeroe Bank Channel are dominated by the relatively warm and salty (S>35) AW entering the region, and below this the cold overflow water exiting to the North Atlantic prevails. Station 143 in the southern Norwegian Basin is to the west of the Atlantic inflow which turns sharply east after crossing over the Iceland-Faeroe Ridge, thus salinities do not exceed 35 at this station. The upper part

of this station has salinities in excess of 34.95 and captures the Recirculated Faeroe Current. This current carries AW that has recirculated and been mixed with ArIW in the Norwegian Basin. The lens of water with S<34.9 between 400 and 600 meter is Norwegian Sea Arctic Intermediate Water (NSArIW), and NSDW dominates below this. The AW is re-encountered at the next stations, 144 and 145, and it reaches its deepest extent at the latter of these, in the Lofoten Basin. NSArIW is present at both of these stations as well, as a salinity minimum at 700 and 1000 m, respectively, and below this NSDW prevails. The sharp gradient in salinity over the Mohns Ridge at stations 146 and 147 is the Arctic Front, north of which the increased influence of PW is manifest as a substantial freshening above 1000 m. The Greenland Sea appears otherwise quite homogenous with respect to both temperature and salinity, but then again we stress that the resolutions applied for salinity and temperature data are inadequate to resolve the fine-scale structures. As the section moves northward through station 149 over the Boreas Basin and then turns east onto the West Spitsbergen shelf, the increasing Atlantic influence at intermediate depths becomes evident with salinities ranging from 34.9 up to 35. Surface waters, though, are quite fresh throughout. In the Boreas Basin, this is due to PW and particularly when close to the shelf it is due to the West Spitsbergen Coastal Current, a continuation of the East Spitsbergen Current that carries water from the northern Barents Sea.

4. Results

4.1 Anthropogenic CO_2 Increase.

The estimated change in anthropogenic CO_2 concentration along the TTO section between 1981 and 2002/03 is displayed in Figure 6. The largest variations of ΔC_{ant} are evident in the upper 100 m. This approximately represents the seasonal mixed layer and is the zone with the largest methodological uncertainty (± 10 μmol kg^{-1}). These estimates should be interpreted

with care and have been shaded gray in the figure. Below this ΔC_{ant} values range from less than 4 μmol kg^{-1} to more than 20 μmol kg^{-1} with systematic spatial variations that are fairly coherent with the water mass distribution. The largest values are associated with the Atlantic domain of the Nordic seas. In the core of the Atlantic inflow, above 600 m in the FBC, ΔC_{ant} lies between 18 and 20 μmol kg^{-1}. This corresponds to annual changes of around 0.9 μmol kg^{-1} yr^{-1}. The ΔC_{ant} decreases slightly moving into the Norwegian Sea but values are clearly higher here than in the rest of the section; in the AW at stations 144 and 145 as well as in the recirculated AW of station 143 values are between 14 and 18 μmol kg^{-1}, corresponding to annual changes of 0.7 to 0.8 μmol kg^{-1} yr^{-1}. The values decrease with depth and in the NSDW ΔC_{ant} is less than 6 μmol kg^{-1}. The isolines in the Norwegian Sea slope northwards and are deepest in the Lofoten Basin where also the Atlantic layer is deepest. The overflow water in the Faeroe Bank Channel has ΔC_{ant} values in the same range as the upper NSDW, between 8 and 10 μmol kg^{-1}. Similar to salinity, ΔC_{ant} decreases sharply across the Arctic Front over the Mohns Ridge and the surface to deep ocean ΔC_{ant} gradient is smallest in the Greenland Sea as a result of deep convective mixing in this region. Approaching the West Spitsbergen Shelf where the influence of AW increase, the ΔC_{ant} lies between 12 and 14 μmol kg^{-1}.

4.2 Anthropogenic $\delta^{13}C$ Changes.

The estimated changes of $\delta^{13}C$ attributable to the oceanic ^{13}C Suess effect, $\Delta\delta^{13}C_{ant}$, are displayed in Figure 7. The deep parts of the Norwegian Basin and most of the Faeroe Bank Channel are excluded as they were outside the common validity range of the $\delta^{13}C$ equations. There are less surface samples, so the contours are not drawn all the way to the surface.

The 1981 to 2003 oceanic ^{13}C Suess effect exhibits substantial regional variation in the Nordic seas, and appears to be even more closely tied to water mass distribution than

anthropogenic CO_2. In the core of the AW in the northern Norwegian Basin and the Lofoten Basin the $\delta^{13}C$ decrease ranges between -0.4‰ and -0.6‰, and corresponds to annual decreases between -0.018‰ yr^{-1} and -0.024‰ yr^{-1}. The changes are smaller in the Greenland Sea, only -0.1‰ which corresponds to -0.004‰ yr^{-1}. As the AW is re-encountered west of Spitsbergen larger changes are evident; between -0.3‰ and -0.4‰.

5. Discussion

The results on the changes of anthropogenic CO_2 concentration and the ^{13}C Suess effect over the last 20 years, the magnitude of these changes, and their spatial variation and relation to water mass distribution provides a framework that enables us to specify how anthropogenic CO_2 is brought into the Nordic seas.

The atmospheric $\delta^{13}C$ has decreased at a fairly steady rate of -0.027‰ yr^{-1} since at least 1962 up to 2003 (calculated from the Southern hemisphere record of *Francey et al*. [1999], extended with the record from the Cape Grim Observatory [*Vaughn and White*, personal communication, 2005].). The $\delta^{13}C$ decreased in the AW by up to -0.024‰ yr^{-1}, so this water mass is close to equilibrium with the atmospheric ^{13}C Suess effect. However, this equilibrium cannot have been established solely within the Nordic seas because it takes ten to twelve years to establish isotopic equilibrium between ocean and atmosphere [*Broecker and Peng*, 1974; *Lynch-Stieglitz et al*., 1995] so the transit time of about 1 year from the Iceland-Scotland gap up to the Lofoten Basin [*Furevik*, 2000; *Furevik*, 2001] is insufficient. Thus the changes must have been advected laterally from further south. The AW has been given time to equilibrate with the atmosphere as it travels towards the Nordic seas via the Gulf Stream–North Atlantic Current–North Atlantic Drift system. Although a large CO_2 uptake within the Nordic seas would preferentially introduce isotopically light carbon to the ocean due to kinetic fractionation [*Lynch-Stieglitz et al*., 1995], the Ct change of 15 to 20 μmol kg^{-1} means that

this kinetic effect can only account for a total decrease of around -0.06‰ (assuming starting conditions of Ct of 2160 μmol kg^{-1} at $\delta^{13}C$ of -1‰, and a one-way addition of 15 μmol kg^{-1} CO_2 at -10‰). The present estimates for the AW ^{13}C Suess effect are similar to what has been seen upstream of the Nordic seas. *Körtzinger et al.* [2003] found a mean ^{13}C Suess effect of -0.026‰ yr^{-1} between 35ºN and 60ºN using isopycnal analysis, and annual changes at Hydrostation S close to Bermuda have been estimated to -0.025‰ yr^{-1} [*Bacastow et al*., 1996; *Gruber et al*., 1999].

As for anthropogenic CO_2 it appears as if the AW goes beyond maintaining equilibrium with the atmosphere because the pCO_2 growth rate in this water actually exceeds the atmospheric growth rate as based on the equivalent pCO_2 increase displayed in Figure 8. Data from Mauna Loa shows that from 1981 to 2002 the atmospheric CO_2 concentrations increased from 339.9 ppm to 373.1 ppm and further to 375.6 ppm in 2003 [*Keeling and Whorf*, 2005]. This gives an annual mean atmospheric CO_2 increase of 1.6 ppm yr^{-1} over the time span covered by the present study (1981 to 2002/03, 21.5 yrs). A similar trend was observed in data obtained within this time interval at Ocean Weather Station Mike (66°N, 2°E) in the Norwegian Sea [*Tans and Conway*, 2005]. The equivalent pCO_2 increase in the regions dominated by AW in the Nordic Seas appears larger than this. In particular, in the Faeroe Bank Channel the estimated growth rates are above 2 μatm yr^{-1}, and in the most saline layers of the northern Norwegian Basin and the Lofoten Basin they range between 1.6 and 1.8 μatm yr^{-1}. These excessive growth rates appear below the upper 100 m, the seasonal mixed layer. At these depths the error of the ΔC_{ant} estimates was ± 5 μmol kg^{-1} which corresponds to an uncertainty of ± 0.37 μatm yr^{-1} in the estimated growth rates (see caption of Figure 8 for details). This gives a range of probable growth rates in the inflow region of between 1.6 and 2.4 μatm yr^{-1}, and from 1.2 to 2.2 μatm yr^{-1} in the AW further north and so it is not crystal clear that pCO_2 growth rates in the AW are exceeding those of the atmosphere. However, an inspection of the

residuals of the MLR equations revealed no systematic bias with region or water mass properties which could ultimately have resulted in a systematic overestimation of the AW pCO_2 growth rates. Moreover, the ± 0.37 μatm yr^{-1} is a measure of the random error of each individual estimate and so the error in the gridded data presented in Figure 8 is probably smaller since independent random errors tends to cancel each other during averaging. This, and the fact that excessive growth rates have also been observed in the source region for the AW entering the Nordic Seas [*Lefévre et al*., 2003; *Friis et al*., 2005; *Omar & Olsen*, 2006] lead us to conclude that it is highly likely that the pCO_2 growth rates in the AW feeding the Nordic Seas are exceeding those of the atmosphere. Local uptake of anthropogenic CO_2 cannot sustain these growth rates. We suggest that the excessive increase is the manifestation of a negative feedback on the North Atlantic CO_2 solubility pump brought about by the advection and cooling of water loaded with anthropogenic CO_2. This phenomenon can be conceptualized in a number of ways [*Wallace*, 2001; *Anderson and Olsen*, 2002; *Völker et al.*, 2002; *Bellerby et al*., 2005]. We have chosen the following approach. The AW that enters the Nordic seas originates further south. As the water moves northward it is cooled and the increased solubility induces a transfer of CO_2 from the atmosphere to the ocean. This cooling-induced uptake is part of the natural pre-industrial exchange of CO_2 between the ocean and the atmosphere; the CO_2 solubility pump. As a result of the uptake of C_{ant}, the Ct content of the source water from the Gulf Stream system has increased. Assume that the pCO_2 of the warm source waters increases at the same rate as the atmosphere; this implies a given anthropogenic change in Ct. The water moves northward and carbon concentrations increase as a consequence of cooling-induced uptake. When Ct increases, the pCO_2 response for a given increase in Ct becomes larger, i.e., the buffer capacity decreases. Therefore, as the water moves northward the effect on pCO_2 of the given anthropogenic change in Ct increases.

Thus the increase in the south, tracking the atmospheric increase, may bring about changes greater than the atmospheric increase further north.

The anthropogenic changes of both $\delta^{13}C$ and Ct that have been estimated for the AW in the Nordic seas thus indicate that this water mass enters the region pre-equilibrated with the atmosphere. Within the Nordic seas it meets with PW and these two mix. The PW has recently exited from under the Arctic ice and has not been in contact with the contemporary atmosphere for long, so both ΔC_{ant} and $\Delta\delta^{13}C$ are lower for this water mass than for the AW. The mixing with PW dilutes the anthropogenic carbon system signature of the AW, yielding the ties with water mass distribution seen for both ΔC_{ant} and $\Delta\delta^{13}C$ in the Nordic seas. The relationship to water mass is stronger for $\Delta\delta^{13}C$ than for ΔC_{ant} (Figures 6 and 7). Regression of ΔC_{ant} vs. salinity in the upper 1000 to 100 m yielded an r^2 of 0.40, which is much less than the r^2 of 0.80 for $\Delta\delta^{13}C_{ant}$ vs. salinity (not shown). We believe the different strengths of the relationships are the consequence of the uptake of anthropogenic CO_2 from the atmosphere which has increased the initially low ΔC_{ant} of the PW after it has entered the Nordic seas, while the low $\Delta\delta^{13}C_{ant}$ signature has been preserved to a greater extent. This effect is due to the atmosphere-ocean CO_2 equilibration rate being ten times greater than the ^{13}C equilibration rate; only one year is required to equilibrate the surface ocean with respect to atmospheric CO_2 changes whereas ten years are required to equilibrate with respect to ^{13}C changes [*Broecker and Peng*, 1974; *Lynch-Stieglitz et al*., 1995]. Thus it appears as if the influx of PW gives rise to a local sink for anthropogenic CO_2 in the Nordic seas.

One might ask to what extent it is not mixing with deep, rather than Polar Waters, that dilutes the anthropogenic signature of the AW. This is in accordance with the classical view of the northern high latitude anthropogenic CO_2 sink [*Takahashi et al*., 2002], and modeling results [*Orr et al.*, 2001; *Wetzel et al*., 2005]. However the impact of deeper waters appears to be limited. This becomes clear through examining the ratio of the anthropogenic isotopic and

carbon changes, $\Delta Rc = \Delta\delta^{13}C_{ant}/\Delta C_{ant}$. The atmospheric perturbation history of $\delta^{13}C$ and anthropogenic CO_2 has been similar and so one might assume similar oceanic penetration as well. This would imply that the ratio of the changes, i.e., ΔRc should be constant. This theory was invoked by *Heimann and Maier-Reimer* [1996] who, when introducing the "dynamic constraint" method for estimating oceanic uptake of anthropogenic CO_2, determined the global ΔRc to be -0.016‰ (μmol kg $^{-1})^{-1}$. However, because of the different equilibration times of ^{13}C and CO_2, significant spatial variations in ΔRc may arise. In particular, for situations where the surface residence time of a water mass has been inadequate for establishment of isotopic equilibrium the ratio will be less negative than for situations were isotopic equilibrium has been established. In the Southern Ocean, ΔRc was shown to vary between -0.007‰ (μmol kg $^{-1})^{-1}$ for water masses with short surface residence time and down to -0.015‰ (μmol kg $^{-1})^{-1}$ for waters with longer surface residence time [*McNeil et al*., 2001b]. Nordic seas ΔRc estimates are plotted as a function of salinity in Figure 9. They take on a wide range of values and, noticeably, vary as a strong function of salinity above 1000 m. This variation reflects the differences and mixing between the PW and AW as discussed above. The AW, which is the most saline water mass, is characterized by the most negative ΔRc which seems to stabilize at -0.032‰ (μmol kg $^{-1})^{-1}$ at the highest salinity values. The fact that this is similar to the values observed by *Körtzinger et al.* [2003] in the AW upstream of the Nordic seas and close to the value expected for a water mass whose CO_2 and $\delta^{13}C$ changes matches those of the atmosphere corroborates that the AW is equilibrated with the atmosphere when entering the Nordic seas. ΔRc approaches zero as salinity decrease, i.e., as the influence of PW increase. This confirms that the PW has not been exposed to the present atmosphere for very long and so is closer to atmospheric equilibrium with respect to CO_2 than with respect to ^{13}C.

The deeper waters, defined here simply as waters below 1000 m, takes on a wide range of values independent of salinity. We identify three reasons why this is so. Firstly, Nordic seas deep waters are, despite of the small variation of salinity, formed from a variety of water masses at a variety of places. The deep water originates in the Arctic Ocean as well as in the Nordic seas so variations in the magnitude of the ΔRc are to be expected. Secondly, limited and variable atmospheric exposure times for deep waters during convective events will introduce ΔRc variability. Finally, the relative uncertainty of the ΔC_{ant} and $\Delta\delta^{13}C_{ant}$ estimates at these depths is greater. The impact of the deep waters on the variability of ΔRc in the upper 1000 m seems to be limited, as most of the points here lie on the straight line connecting the PW and AW. Only at salinities around 34.9 does this slope seem perturbed by deep mixing with many points higher than the expected value. This is apparently a result of mixing with deeper waters, as these typically have higher ΔRc than what is expected from the PW-AW mixing line. As can be seen from Figure 5, it is only in the homogenous Greenland Sea that these waters reach the surface and support an anthropogenic carbon uptake.

6. Conclusions & Implications

The increase of the anthropogenic carbon concentrations and the $\delta^{13}C$ decrease in the Nordic seas have been quantified using an extended version of the multi-linear regression approach of *Wallace* [1995]. The distribution of the changes and in particular their relationship to each other showed a high dependency on water masses and circulation. This dependency has illuminated the processes that bring anthropogenic CO_2 into the Nordic seas. Firstly, anthropogenic CO_2 is advected into the region with the AW. The isotopic changes were too large to have taken place solely within the Nordic seas where the residence time is only a few years. Advection and cooling of water from further south in the Atlantic provides a reasonable explanation for the excessive pCO_2 increases evident in the core of the AW [*Wallace*, 2001;

Anderson and Olsen, 2002]. The large negative ΔRc values of the AW corroborate this view; they reflect that the water has been exposed to the present atmosphere for a considerable time and are similar to the ΔRc values observed by *Körtzinger et al.* [2003] south of the Scotland-Greenland ridge. Secondly, and in contrast to the AW, in the PW the anthropogenic CO_2 changes are relatively large compared to the isotopic changes, perhaps best reflected in the trend of increasing ΔRc with decreasing salinity. This observation and the fact that the PW exits from under the Arctic ice imply that the influx of PW promotes an uptake of anthropogenic CO_2 from the atmosphere within the Nordic seas. Finally, convection in the Greenland Sea does seem to lead to surfacing of deep water which takes up anthropogenic CO_2 from the atmosphere.

Given this, we expect that the air-sea flux of anthropogenic CO_2 in the Nordic seas exhibits a distinct spatial pattern that is intimately linked to surface water mass distribution. In the eastern part, the Atlantic region, the uptake of C_{ant} from the atmosphere is probably limited, if not even negative; that is, it may be a source of anthropogenic CO_2 to the atmosphere. This latter phenomenon would be apparent as a decreased undersaturation compared to pre-industrial times. Our findings indicate that the undersaturation has decreased at least over the last two decades. The area towards the west, on the other hand, across the Arctic Front, is most likely a sink of anthropogenic CO_2 from the atmosphere as the surface waters of this region are appreciably influenced by PW and deep mixing. This feature, i.e., a quasi-meridional gradient approximately following the position of the Arctic Front is not evident in estimates of the air-sea flux of anthropogenic CO_2 from coarse-resolution ocean carbon model runs. There are discrepancies between different models, but most of them seem to agree that there is a basin-wide uptake of anthropogenic CO_2 in the Nordic seas [*Orr et al*., 2001; *Wetzel et al*., 2005]. This flux is brought about by deep water formation in the models [*Wetzel et al.*, 2005]. The difference between our inferred spatial pattern and model output supports the need

for instance for better spatial resolution and improved representation of convective processes in order for models to properly reproduce oceanic uptake of anthropogenic CO_2.

When collapsing pCO_2 data collected over a number of years to a 1995 climatology *Takahashi et al.* [2002] assumed no temporal trend of surface ocean pCO_2 north of 45°N in the Atlantic. They argued that the anthropogenic signal in surface ocean pCO_2 in the region should be completely diluted by deep mixing. On the other hand *Olsen et al.* [2003] assumed that the whole region followed the atmospheric pCO_2 increase. Our results show that neither of these assumptions are totally correct. *Olsen et al.* [2003] appear closer to the truth than *Takahashi et al*. [2002] but the temporal evolution of surface ocean pCO_2 differs from region to region. The limited spatial coverage of the TTO data and increased random uncertainty of the ΔC_{ant} estimates in the upper 100 m prohibit a comprehensive analysis, but as a first order estimate we suggest that the annual pCO_2 increase varies as function of salinity according to: $\Delta pCO_2 = 2.074 \times S - 71.13$, $r^2 = 0.6$, n = 76, rms = 0.2. This equation was derived through the linear regression of the annual pCO_2 increase as estimated for Figure 8 and salinity in the upper 500 to 100 m. 100 m was used as the upper cut off because of the increased random uncertainty of the ΔC_{ant} estimates shallower than this.

The ratio of the anthropogenic isotopic and CO_2 changes, ΔRc has been used as a conversion factor to get from estimates of the oceanic ^{13}C Suess effect to anthropogenic CO_2 estimates. Several authors have multiplied their estimates of $\delta^{13}C$ changes by -0.016‰ (μmol kg $^{-1}$)$^{-1}$, the ΔRc estimate of *Heimann and Maier-Reimer* [1996], to get to C_{ant} estimates [*Bauch et al.*, 2000; *Ortiz et al*., 2000]. This procedure cannot be recommended since different surface residence times of water masses produce substantial variations in ΔRc at regional scales, as was also shown by *McNeil et al.* [2001b] for the Southern Ocean. The ΔRc values of the AW are exceptional, and much more negative than the values determined by *Tanaka et al*. [2003] at 44°N in the Pacific. This reflects the special circulation of the Atlantic. *Tanaka et al*.

[2003] suggested that their value was applicable in general in subpolar and polar regions; this is not correct.

The present findings support the results of anthropogenic carbon transport calculations in that the AW brings with it a large amount of anthropogenic CO_2 to the northern North Atlantic [*Álvarez et al*., 2003; *Macdonald et al*., 2003; *Rosón et al*., 2003]. In particular *Álvarez et al.* [2003] estimated that 56% of the anthropogenic carbon sequestered north of 24.5°N was brought in by oceanic transport whereas 44% was taken up from the atmosphere within the region. Just how large the ratio is in the Nordic seas has yet to be determined, but the advective flux must be significant. Given our findings it is reasonable to assume that the AW is saturated with anthropogenic CO_2. Temperature and TA of the AW entering the Nordic seas is around 8°C and 2325 μmol kg^{-1}, respectively; this gives a total anthropogenic CO_2 concentration of ~53 μmol kg^{-1} (atmospheric pCO_2 280 μatm vs. 380 μatm) which is reasonable compared to *Körtzinger et al.* [1998]. About 6 Sv overturn in the Nordic seas [*Hansen and Østerhus*, 2000]. Combining these numbers we estimate that overturning leads to an annual sequestration of roughly 0.12 Gt C_{ant} in the Nordic seas. This is 6% of the annual oceanic accumulation of 1.8 Gt C_{ant} [*Prentice et al.*, 2001]. Future studies should elaborate our initial, conceptual appraisal of how mixing with PW dilutes the anthropogenic carbon system signature of the AW within the Nordic Seas and quantify the relative importance of air-sea fluxes and oceanic transport for importing anthropogenic carbon into the region.

What we'd finally like to emphasize here is the fact that the C_{ant} transport can bring around the excessive pCO_2 increase seen in the core of the AW [*Anderson and Olsen*, 2002, *Wallace*, 2001]. Similar large increases have been seen further south by *Lefévre et al*. [2004], *Friis et al*. [2005], and *Omar and Olsen* [2006]. This gives us reason to believe that the AW feature is the northernmost manifestation of a trend that occurs in all regions fed with water from the

Gulf Stream; that is, surface pCO_2 levels in the whole North Atlantic Drift–Norwegian Atlantic Current system are currently approaching equilibrium with the atmosphere.

Acknowledgements

Financial support from the EU through IP CARBOOCEAN (511176-2) and TRACTOR (EVK2-2000-00080) is greatly appreciated. The Cape Grim Observatory $\delta^{13}C$ record from 1991 to 2003 was kindly provided by Dr. Bruce H. Vaughn and Dr. James W.C. White at the Institute of Arctic and Alpine Research, University of Colorado. The authors would like to thank the officers and crews of R/V *Knorr* and R/V *G.O. Sars* and the chief scientists of the *Knorr* cruise, Dr. Jim Swift and Dr. Bill Smethie for their cooperation and organization. Dr. Yoshie Kasajima kindly provided the *Sars* temperature and salinity data, and Dr. Jim Swift kindly provided the *Knorr* temperature, salinity, and nutrients data. James Orr and Rolf Sonnerup provided thorough, intelligent and helpful comments on the manuscript. This is contribution A 131 from the Bjerknes Centre for Climate Research.

References

Aminot, A., and R. Kérouel (1998), Pasteurization as an alternative method for preservation of nitrate and nitrite in seawater samples, *Mar. Chem.*, *61*, 203-208.

Álvarez, M., A.F. Rios, F.F. Pérez, H.L. Bryden, and G. Rosón (2003), Transports and budgets of total inorganic carbon in the subpolar and temperate North Atlantic, *Global Biogeochem. Cyles*, *17*(1), 1002, doi: 10.1029/2002GB001881.

Álvarez, M., H.L. Bryden, F.F. Pérez, A.F. Rios, and G. Rosón (2002), Physical and biogeochemical fluxes and net budgets in the subpolar and temperate North Atlantic, *J. Mar. Res.*, *60*, 191-226.

Anderson L.G. and A. Olsen (2002), Air-sea flux of anthropogenic carbon dioxide in the North Atlantic, *Geophys. Res. Lett.*, *29*(17), 1835, doi: 10.1029/2002GL014820.

Bacastow, R.B., C.D. Keeling, T.J. Lueker, M. Wahlen, and W.G. Mook (1996), The $\delta^{13}C$ Suess effect in the world surface oceans and its implications for oceanic uptake of CO_2: Analysis of observations at Bermuda, *Global Biogeochem. Cycles*, *10*, 335-346.

Bauch, D., J. Carstens, G. Wefer, and J. Thiede (2000), The imprint of anthropogenic CO_2 in the Arctic Ocean: evidence from planktic $\delta^{13}C$ data from watercolumn and sediment surfaces, *Deep-sea Res*. *II*, *47*, 1791-1808.

Bellerby, R.G.J, A. Olsen, T. Furevik, and L.G. Anderson (2005), Response of the surface ocean CO_2 system in the Nordic seas and northern North Atlantic to climate change, in *The Nordic seas, an integrated perspective, Geophys. Monogr. Ser.*, vol. 158, edited by H. Drange, T. Dokken, T. Furevik, R. Gerdes, and W. Berger, pp. 189-197, AGU, Washington D.C., USA, 2005.

Blindheim, J. and Østerhus, S., The Nordic seas, Main Oceanographic Features (2005), in *The Nordic seas, an integrated perspective, Geophys. Monogr. Ser.*, vol. 158, edited by H.

Drange, T. Dokken, T. Furevik, R. Gerdes, and W. Berger, pp. 11-37 AGU, Washington D.C., USA.

Brewer, P.G., T. Takahashi, and R.T. Williams (1986), Transient tracers in the ocean - hydrography data and carbon dioxide systems with revised carbon chemistry data. NDP-004/R1, Carbon Dioxide Analysis Information Center (CDIAC), Oak Ridge National Laboratory, Oak Ridge, Tennessee.

Broecker, W.S., and T.-H. Peng (1974), Gas exchange rates between air and sea, *Tellus*, *26*, 21-35.

Dickson, A.G. and J.P. Riley (1978), The effect of analytical error on the evaluation of the components of the aquatic carbon-dioxide system, *Mar. Chem.*, *6*, 77-85.

Falck, E., and L.G. Anderson (2005), The dynamics of the carbon cycle in the surface water of the Norwegian Sea, *Mar. Chem. 94*, 43-53.

Francey, R.J., C.E. Allison, D.M. Etheridge, C.M. Trudinger, I.G. Enting, M. Leuenberger, R.L. Langefelds, E. Michel, and L.P. Steele (1999), A 1000-year high precision record of $\delta^{13}C$ in atmospheric CO_2, *Tellus*, *51B*, 170-193.

Friis, K., A. Körtzinger, J. Pätsch, and D.W.R. Wallace (2005), On the temporal increase of anthropogenic CO_2 in the subpolar North Atlantic, *Deep-Sea Res. I*, 52, 681-698.

Furevik, T. (2001), Annual and interannual variability of the Atlantic Water temperatures in the Norwegian and Barents Seas: 1980-1996 , *Deep-Sea Res. I*, *48*, 383-404.

Furevik, T. (2000), On anomalous sea surface temperatures in the Nordic Seas , *J. Clim.*, *13*, 1044-1053.

Grasshoff, K. (1970), A simultaneous multiple channel system for nutrient analysis in seawater with analog and digital data record, *Tecnicon Qtrly*, *3*, 7-17.

Gruber, N., C.D. Keeling, R.B. Bacastow, P.R. Guenther, T.J. Lueker, M. Wahlen, H.A.J. Meijer, W.G. Mook, and T.F. Stocker (1999), Spatiotemporal patterns of carbon-13 in

the global surface oceans and the oceanic Suess effect, *Global Biogeochem. Cycles*, *13*, 307-335.

Gruber, N. (1998), Anthropogenic CO_2 in the Atlantic Ocean, *Global Biogeochem. Cycles*, *12*, 165-191.

Gruber, N., J.L. Sarmiento, and T.F. Stocker (1996), An improved method for detecting anthropogenic CO_2 in the oceans, *Global Biogeochem. Cycles*, *10*, 809-837.

Hansen, B. and S. Østerhus (2000), North Atlantic-Nordic Seas exchanges, *Prog. Oceanogr.*, *45*, 109-208.

Heimann, M., and E. Maier-Reimer (1996), On the relations between the oceanic uptake of CO_2 and its carbon isotopes, *Global Biogeochem. Cycles*, *10*, 89-110.

Hopkins, T.S. (1991), The GIN Sea - A synthesis of its physical oceanography and literature review 1972-1985, *Earth-Sci. Rev.*, *30*, 175-318.

Johnson, K.M., A.E. King, and J.M. Sieburth (1985), Coulometric TCO_2 analyses for marine studies: An introduction, *Mar. Chem.*, *16*, 61-82.

Johnson, K.M., J.M. Sieburth, P.J. Williams, and L. Brandstrom (1987), Coulometric total carbon dioxide analysis for marine studies: Automation and calibration, *Mar. Chem.*, *21*, 117-133.

Keeling, C.D. and T.P. Whorf (2005), Atmospheric CO_2 records from sites in the SIO air sampling network, in *Trends: A Compendium of Data on Global Change*, Carbon Dioxide Information Analysis Center, Oak Ridge National Laboratory, U.S. Department of Energy, Oak Ridge, Tenn., U.S.A..

Körtzinger, A., P.D. Quay, and R.E. Sonnerup (2003), Relationship between anthropogenic CO_2 and the ^{13}C Suess effect in the North Atlantic Ocean, *Global Biogeochem. Cycles*, *17*, 1005, doi: 10.1029/2001GB001427.

Körtzinger, A., L. Mintrop, J.C. Duinker (1998), On the penetration of anthropogenic CO_2 into the North Atlantic Ocean, *J. Geophys. Res.*, *103*, 18681-18689.

Lefévre, N., A. J. Watson, A. Olsen, A.F. Ríos, F.F., Pérez, and T. Johannessen (2004), A decrease in the sink for atmospheric CO_2 in the North Atlantic, *Geophys. Res. Lett.*, *31*, L07306, doi: 10.1029/2003GL018957.

Lynch-Stieglitz, J., T.F. Stocker, W.S. Broecker, and R. G. Fairbanks (1995), The influence of air-sea exchange on the isotopic composition of oceanic carbon: Observations and modelling, *Global Biogeochem. Cycles*, *9*, 653-665.

Macdonald, A.M., M.O. Baringer, R. Wanninkhof, K.L. Lee, and D.W.R. Wallace (2003), A 1998-1992 comparison of inorganic carbon and its transport across 24.5ºN in the Atlantic, *Deep-Sea Res. II*, *50*, 3041-3064.

McNeil, B.I., B. Tilbrook, and R.J. Matear (2001a), Accumulation and uptake of anthropogenic CO_2 in the Southern Ocean, south of Australia between 1968 and 1996, *J. Geophys. Res*., *106*, 31431-31445.

McNeil, B.I., R.J. Matear, and B. Tilbrook (2001b), Does carbon 13 track anthropogenic CO_2 in the Southern Ocean?, *Global Biogeochem. Cycles.*, *15*, 597-613.

Merbach, C., C.H. Culberson, J.E. Hawley, and R.M. Pytkowicz (1973), Measurement of apparent dissociation constants of carbonic acid in seawater at atmospheric pressure, *Limn. and Oceanogr.*, *18*, 533-541.

Murphy, J. and J.P. Riley (1962), A modified single solution method for the determination of phosphate in natural waters. *Anal. Chim. Acta*, *27*, 31-36.

Nondal, G. (2004), The carbon dioxide system in the northern North Atlantic: an assessment of the optimal variable combination for voluntary observing ships. M.S. thesis, 71 pp., Univ. of Bergen, Bergen, Norway, 6 Sept.

Olsen, A., R.G.J. Bellerby, T. Johannessen, A.M. Omar, and I. Skjelvan (2003), Interannual variability in the wintertime air-sea flux of carbon dioxide in the northern North Atlantic, 1981-2001, *Deep-Sea Res. I.*, 50, 1323-1338.

Omar, A. M. and A. Olsen (2006), Reconstructing the time history of the air-sea CO_2 disequilibrium and its rate of change in the eastern subpolar North Atlantic, 1972-1989, *Geophys. Res. Lett.*, 33, L04602, doi: 10.1029/2005GL025425.

Omar, A., T. Johannessen, S. Kaltin, and A. Olsen (2003), Anthropogenic increase of oceanic pCO_2 in the Barents Sea surface water, *J. Geophys. Res.*, *108*(C12), 3388, doi: 10.1029/2002JC001628.

Orr, J.C., E. Maier-Reimer, U. Mikolajewicz, P. Monfray, J.L. Sarmiento, J.R. Toggweiler, N.K. Taylor, J. Palmer, N. Gruber, C.L. Sabine, C. Le Quéré, R.M. Key, and J. Boutin (2001), Estimates of anthropogenic carbon uptake from four three-dimensional global ocean models, *Global Biogeochem. Cycles*, *15*, 43-60.

Ortiz, J.D., A.C. Mix, P.A. Wheeler, and R.M. Key (2000), Anthropogenic CO_2 invasion into the northeast Pacific based on concurrent $\delta^{13}C_{DIC}$ and nutrient profiles from the California Current, *Global Biogeochem. Cycles*, *14*, 917-929.

Peng, T.-H., R. Wanninkhof, and R.A. Feely (2003), Increase of anthropogenic CO_2 in the Pacific Ocean over the last two decades, *Deep-Sea Res. II*, *50*, 3065-3082.

Peng, T.-H., R. Wanninkhof, J.L. Bullister, R.A. Feely, and T. Takahashi (1998), Quantification of decadal anthropogenic CO_2 uptake in the ocean based on dissolved inorganic carbon measurements, *Nature*, *396*, 560-563.

Prentice, I.C. C.D. Fraquahar, M.J.R. Fasham, M.L. Goulden, M. Heimann, V.J. Jaramillo, H.S. Kheshgi, C. Le Quéré, R.J. Scholes, and D.W.R. Wallace (2001), The carbon cycle and atmospheric carbon dioxide, in *Climate change 2001: the scientific basis. Contribution of Working Group I to the Third Assessment Report of the*

Intergovernmental Panel on Climate change, edited by J.T. Houghton, Y. Ding, D.J. Griggs, M. Noguer, P.J. van de Linden, X. Dai, K. Maskell, and C.A. Johnson, pp. 183-237, Cambridge University Press, Cambridge, United Kingdom and New York, NY, USA.

Quay, P, R. Sonnerup, T. Westby, J. Strutsman, and A. McNichol (2003), Changes in the $^{13}C/^{12}C$ of dissolved inorganic carbon as a tracer for anthropogenic CO_2 uptake, *Global Biogeochem. Cycles*, *17*, 1004, doi: 10.1029/2001GB001817.

Quay, P.D, B. Tilbrook, and C.S. Wong (1992), Oceanic uptake of fossil fuel CO_2: Carbon-13 evidence, *Science*, *256*, 74-79.

R Development Core Team (2004), R: A language and environment for statistical computing. R Foundation for Statistical Computing, Vienna, Austria. ISBN 3-900051-07-0, URL http://www.R-project.org.

Rosón, G., A.F. Rios, F.F. Pérez, A. Lavin, and H.L. Bryden (2003), Carbon distribution, fluxes, and budgets in the subtropical North Atlantic Ocean, *J. Geophys. Res*., *108*, 3144, doi:10.1029/1999JC000047.

Rudels, B., G. Björk, J. Nilson, P. Winsor, I. Lake, and C. Nohr (2005), The interaction between waters from the Arctic Ocean and the Nordic Seas north of the Fram Strait and along the East Greenland Current: results from the Arctic Ocean-02 Oden expedition, *J. Mar. Sys.*, *55*, 1-30.

Sabine, C.L., R.A. Feely, N. Gruber, R.M. Key, K. Lee, J.L. Bullister, R. Wanninkhof, C.S. Wong, D.W.R. Wallace, B. Tilbrook, F.J. Millero, T.-H. Peng, A. Kozyr, T. Ono, A.F. Rios (2004), The oceanic sink for anthropogenic CO_2, *Science*, *305*, 367-371.

Sabine, C., R.M. Key, K.M. Johnson, F.J. Millero, A. Poisson, J.L. Sarmiento, D.W.R. Wallace, and C.D. Winn (1999), Anthropogenic CO_2 inventory in the Indian Ocean, *Global Biogeochem, Cycles*, *13*, 179-198.

Sonnerup, R.E., P.D. Quay, and A.P. McNichol (2000), The Indian Ocean ^{13}C Suess effect, *Global Biogeochem. Cycles*, *14*, 903-916.

Tanaka, T., Y.W. Watanabe, S. Watanabe, S. Noriki, N. Tsurushima, and Y. Nojiri (2003), Oceanic Suess effect of $\delta^{13}C$ in subpolar region: The North Pacific, *Geophys. Res. Lett.*, *30*(22), 2159, doi: 10.1029/2003GL018503.

Tanhua, T., and D.W.R. Wallace (2005), Consistency of TTO-NAS inorganic carbon data with modern measurements. *Geophys. Res. Lett.*, 32, L14618, doi:10.1029/2005GL023248.

Tans, P.P. and T.J. Conway (2005), Monthly atmospheric CO_2 mixing rations from the NOAA CMDL Carbon Cycle Cooperative Global Air Sampling Network, 1968-2002, in *Trends: A Compendium of Data on Global Change*, Carbon Dioxide Information Analysis Center, Oak Ridge National Laboratory, U.S. Department of Energy, Oak Ridge, Tenn., U.S.A..

Tans, P.P., J.A. Berry, and R.F. Keeling (1993), Oceanic $^{13}C/^{12}C$ uptake observations: A new window on ocean CO_2 uptake, *Global Biogeochem. Cycles*, *14*, 353-368.

Takahashi, T., S.C. Sutherland, C. Sweeney, A. Poisson, N. Metzl, B. Tilbrook, N. Bates, R. Wanninkhof, R.A. Feely, C. Sabine, J. Olafsson, and Y. Nojiri (2002), Global sea-air CO_2 flux based on climatological surface ocean pCO_2, and seasonal biological and temperature effects, *Deep-Sea Res II*, *49*, 1601-1622.

Völker, C., D.W.R. Wallace, and D.A. Wolf-Gladrow (2002), On the role of heat fluxes in the uptake of anthropogenic carbon in the North Atlantic, *Global Biogeochem. Cycles*, *16*(4), 1138, doi: 10.1029/2002GB001897.

Wallace, D.W.R. (2001), Storage and transport of excess CO_2 in the oceans, in: The JGOFS/WOCE global CO_2 survey, in *Ocean circulation and climate: observing and*

modelling the global ocean, edited by G. Siedler, J. Church, and J. Gould, 489-521, Academic Press, London, 2001

Wallace, D.W.R. (1995), Monitoring global ocean carbon inventories, *OOSDP Backgound Rep. 5*, 54 pp. Ocean Observ. System Dev. Panel, Texas A&M Univ., College Station, TX, USA.

Weiss, R.F., R.A. Janke, and C.D. Keeling (1982), Seasonal effects of temperature and salinity on the partial pressure of CO_2 in sea water, *Nature 300*, 511-513.

Wells, D.E. and W.P. Cofino (1997), A review of the achievents of the EU project 'QUASIMEME' 1993-1996, *Marine Pollution Bulletin*, *35*, 3-17.

Wetzel, P., A. Winguth, and E. Maier-Reimer (2005), Sea-to-air CO_2 flux from 1948 to 2003: A model study, *Global Biogeochem. Cycles*, *19*, doi: 10.1029/2004GB002339

Figure Captions

1. Map of the sampling locations in the Nordic seas. The TTO sampling locations are shown as crosses, *Knorr* locations as solid circles, and *Sars* locations as open diamonds. The thin lines mark the position of the 250 m isobath.

2. Residuals (measured - predicted) of Ct (a) and $\delta^{13}C$ (b) as a function of predicted values. Residuals of the *Knorr*/*Sars* regressions as solid circles, and residuals of the TTO regressions as open circles.

3. Mean and standard deviation of residuals of Ct (a) and $\delta^{13}C$ (b) binned into intervals of 0-99 m, 100-199 m, 200-299 m, 300-499 m, and into 500 meter intervals below 500 m. The residuals of the *Knorr*/*Sars* regressions are in black whereas those of the TTO regressions are in grey.

4. Schematic of Nordic seas surface circulation. The solid lines indicate the flow of warm Atlantic Water and the dashed lines show the flow of the cold Polar Water. The gray dotted line shows the position of the section given in Figure 5-8, along with the location (crosses) and numbers of the TTO stations used for its construction.

5. TTO data based sections of temperature (a) and salinity (b) from the Faeroe Bank Channel to the West Spitsbergen Shelf along the track shown in Figure 4. The numbers on the upper x-axis refer to the station numbers in Figure 4.

6. Estimated anthropogenic CO_2 increase (μmol kg^{-1}) in the Nordic seas from 1981 to 2002/03, along the track shown in Figure 4. The numbers on the upper x-axis refer to the station numbers in Figure 4. The gray shading of the upper 100 m indicates the higher uncertainty of the ΔC_{ant} estimates in this depth range (10 μmol kg^{-1} compared to 5 μmol kg^{-1} elsewhere).

7. Estimated $\delta^{13}C$ change (‰) attributable to the oceanic ^{13}C Suess effect in the Nordic seas from 1981 to 2003, along the track shown in Figure 4. The numbers on the upper x-axis refer to the station numbers in Figure 4.

8. Equivalent pCO_2 growth rate in the Nordic seas 1981-2002/03 (μatm yr^{-1}), along the track shown in Figure 4. The numbers on the upper x-axis refer to the station numbers in Figure 4. The growth rate was computed as the mean annual increase in CO_2 partial pressure required to increase the TTO Ct data by the estimated anthropogenic increase if at surface, i.e. $[pCO_2(Ct^{TTO}+\Delta C_{ant}, At^0, P,\theta, S, Si, PO_4) - pCO_2(Ct^{TTO}, At^0, P, \theta, S, Si, PO_4)]/21.5$, where preformed alkalinity (At^0) was determined according to *Nondal* [2004], pressure (P) was set to zero, θ and S are in situ potential temperature and salinity, and Si and PO_4 were set constant to 8 and 1, respectively (typical wintertime conditions). The error of the growth rate estimates was determined to ± 0.64 μatm yr^{-1} in the upper 100 m and ± 0.37 μatm yr^{-1} elsewhere by propagating the random error associated with ΔC_{ant} (± 10 and ± 5 μmol kg^{-1}, respectively, section 2.4) according to Dickson and Riley (1978). Errors in the other variables used for pCO_2 determination including dissociation constants, were not considered because these have the same effect on two pCO_2 estimates and thus cancel out as the difference is computed.

9. Ratio of 1981-2002/03 Nordic seas anthropogenic $\delta^{13}C$ and Ct changes ($\Delta Rc = \Delta\delta^{13}C_{ant}/\Delta C_{ant}$) as a function of salinity. Solid circles are data obtained between 100 and 1000 m, open circles are data obtained deeper than 1000 m. The line shows the linear regression in the 100 to 1000 m depth range, $r^2 = 0.93$.

Table 1. Regression coefficients and statistics for the predictive equations which were of the form: $Ct = a \times S + b \times \theta + c \times NO_3 + d \times Si + k$ and $\delta^{13}C = a \times S + b \times \theta + c \times NO_3 + d \times Si + k$.

Relationship	a	b	c	d	k	r^2	rms	n
1981 Ct	65.0535	-5.9032	3.9031	-0.5033	-170.8064	0.96	5.88	274
1981 $\delta^{13}C$	0.04554	0.07225	-0.02909	0.0138	-0.09162	0.98	0.062	18
2002/03 Ct	18.75019	-3.2875	5.83105	-2.18864	1442.3472	0.95	4.62	2058
2003 $\delta^{13}C$	-0.574599	0.026418	-0.067470	0.057407	21.594664	0.81	0.070	199

Table 2. Common application ranges of the predictive equations for Ct and for $\delta^{13}C$.

Parameter	range Ct	range $\delta^{13}C$
salinity	34.172-35.249	34.784-35.084
θ	-1.288 - 10.49	-1.15-8.45
nitrate	0.5-15.8	2.74-15.01
silicate	0.2-13.4	0.75-12.25

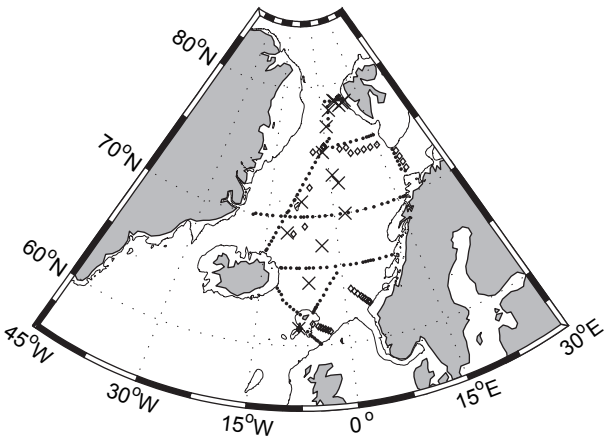
80°N
70°N
60°N
45°W
30°W
15°W
0°
15°E
30°E

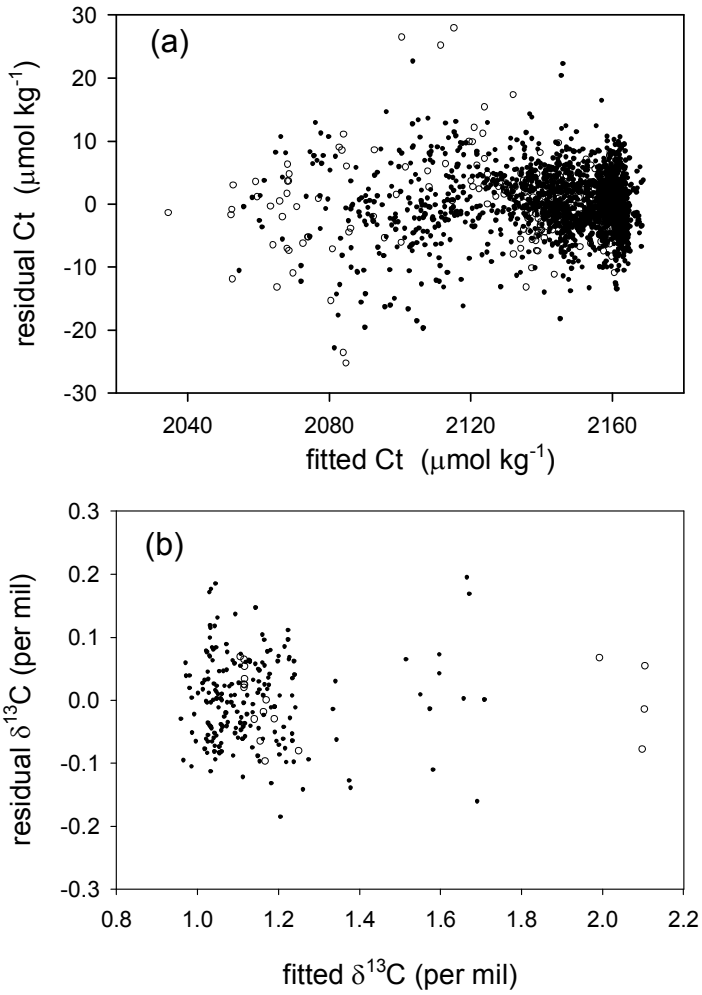
(a)
residual Ct (μmol kg-1)
fitted Ct (μmol kg-1)
30
20
10
0
-10
-20
-30
2040
2080
2120
2160
(b)
residual δ13C (per mil)
fitted δ13C (per mil)
0.3
0.2
0.1
0.0
-0.1
-0.2
-0.3
0.8
1.0
1.2
1.4
1.6
1.8
2.0
2.2

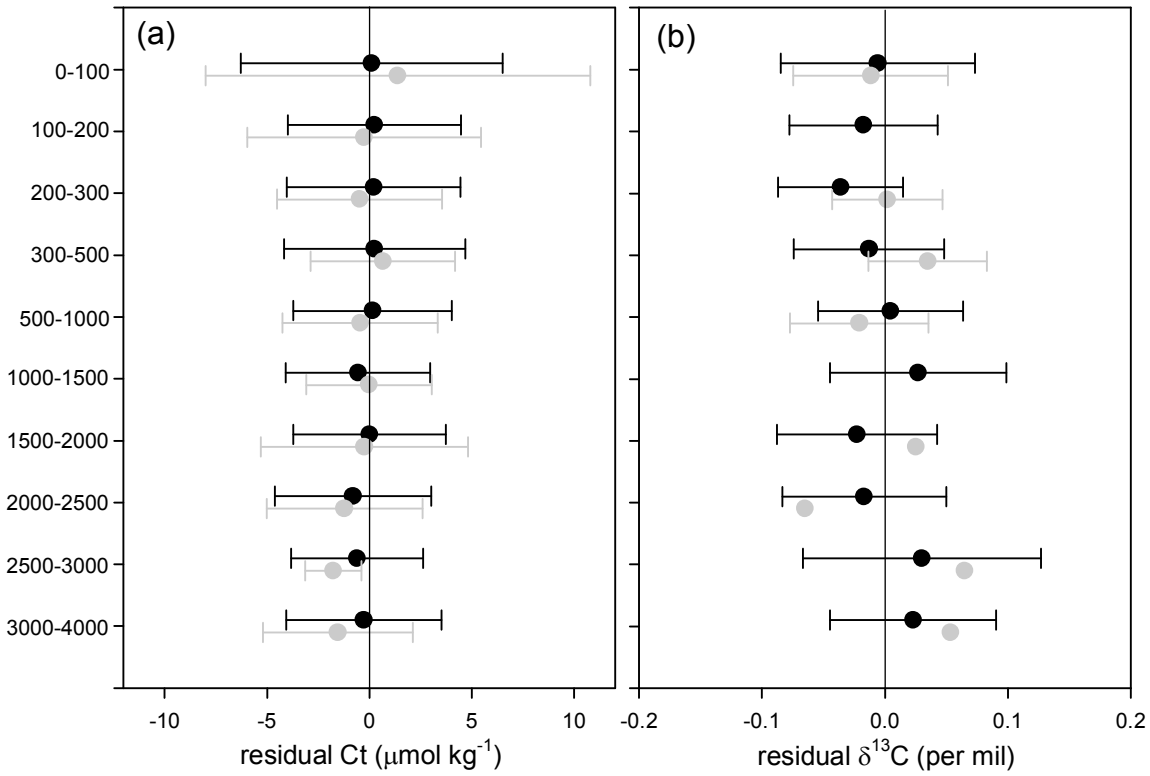
(a)
(b)
0-100
100-200
200-300
300-500
500-1000
1000-1500
1500-2000
2000-2500
2500-3000
3000-4000
-10
-5
0
5
10
-0.2
-0.1
0.0
0.1
0.2
residual Ct (μmol kg-1)
residual δ13C (per mil)

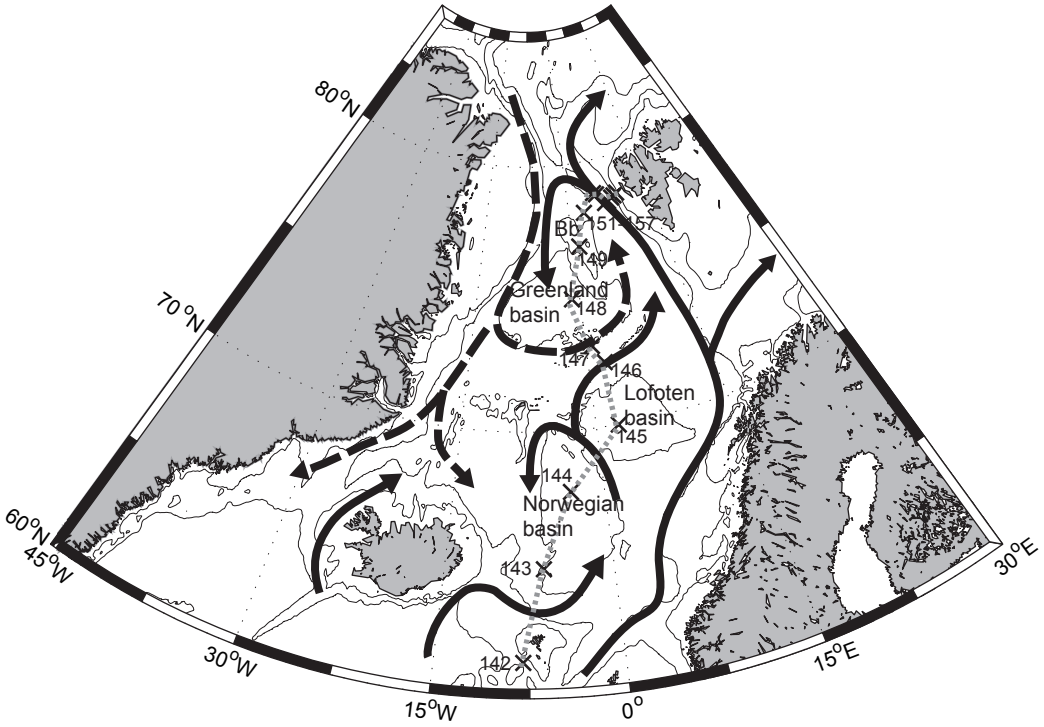
80°N
70°N
60°N
45°W
30°W
15°W
0°
15°E
30°E
Bb
151
157
149
Greenland
basin
148
147
146
Lofoten
basin
145
144
Norwegian
basin
143
142

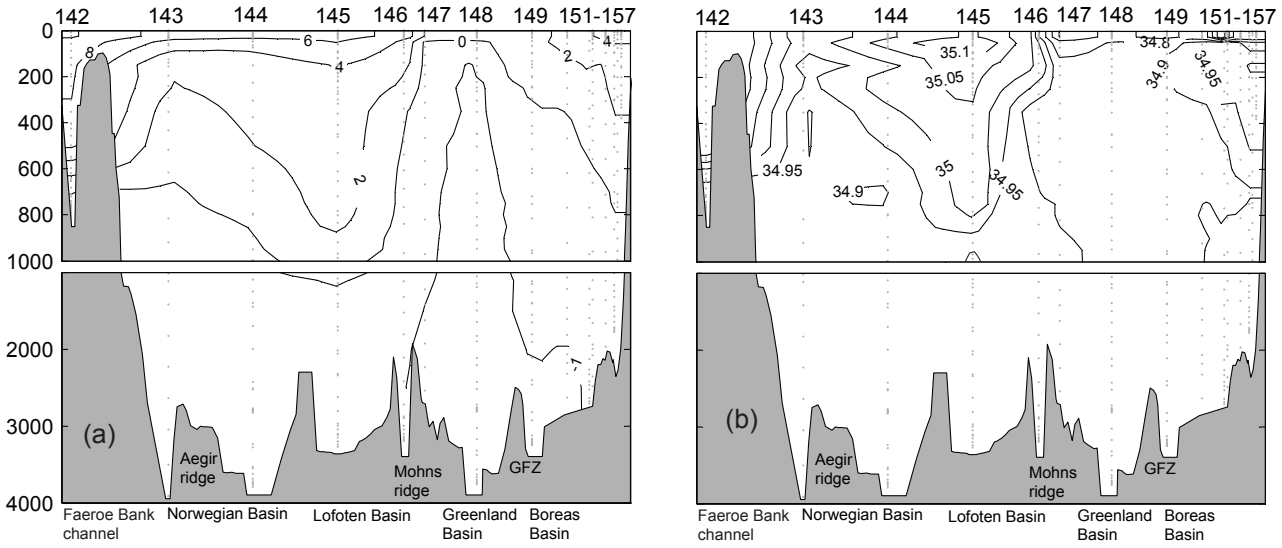
142
143
144
145
146
147
148
149
151-157
0
200
400
600
800
1000
2000
3000
4000
8
6
4
2
0
2
4
(a)
Aegir ridge
Mohns ridge
GFZ
Faeroe Bank channel
Norwegian Basin
Lofoten Basin
Greenland Basin
Boreas Basin
35.1
35.05
34.8
34.9
34.95
35
34.95
34.9
(b)
Aegir ridge
Mohns ridge
GFZ
Faeroe Bank channel
Norwegian Basin
Lofoten Basin
Greenland Basin
Boreas Basin

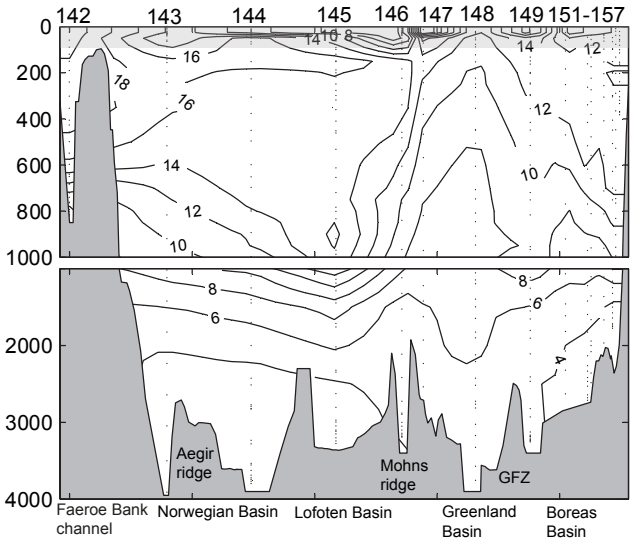
142
143
144
145
146
147
148
149
151-157
0
200
400
600
800
1000
2000
3000
4000
Aegir ridge
Mohns ridge
GFZ
Faeroe Bank channel
Norwegian Basin
Lofoten Basin
Greenland Basin
Boreas Basin

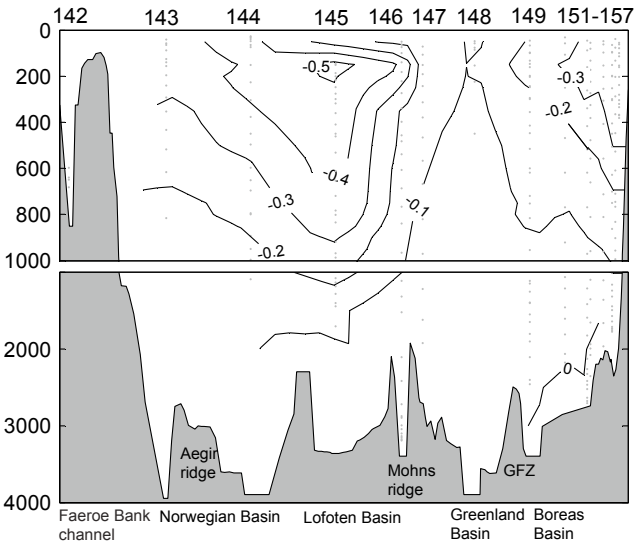
142
143
144
145
146
147
148
149
151-157
0
200
400
600
800
1000
2000
3000
4000
-0.5
-0.4
-0.3
-0.2
-0.7
-0.3
-0.2
0
Aegir ridge
Mohns ridge
GFZ
Faeroe Bank channel
Norwegian Basin
Lofoten Basin
Greenland Basin
Boreas Basin

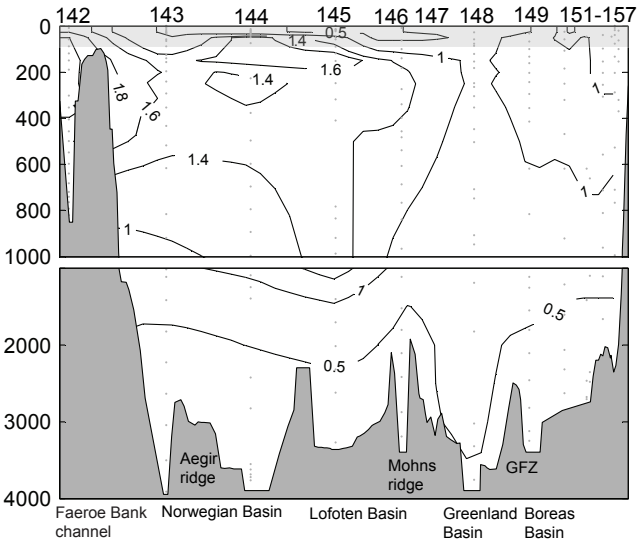
142
143
144
145
146
147
148
149
151-157
0
200
400
600
800
1000
2000
3000
4000
1.8
1.6
1.4
1
0.5
Aegir ridge
Mohns ridge
GFZ
Faeroe Bank channel
Norwegian Basin
Lofoten Basin
Greenland Basin
Boreas Basin

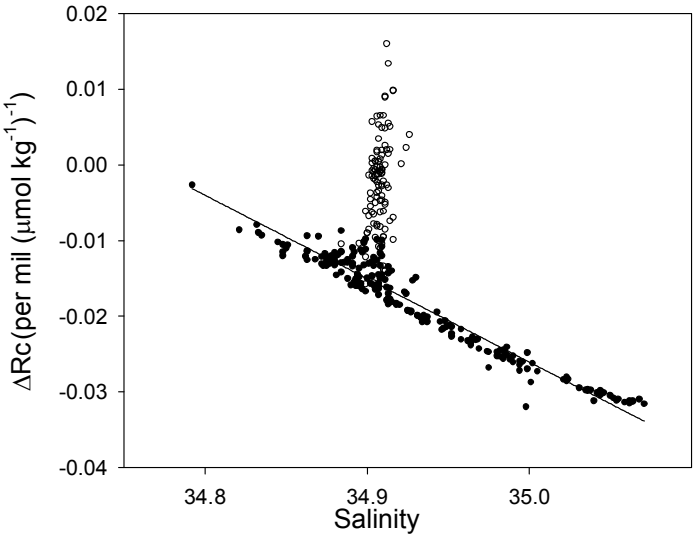
0.02
0.01
0.00
-0.01
-0.02
-0.03
-0.04
ΔRc(per mil (μmol kg-1)-1)
34.8
34.9
35.0
Salinity